

## On Turbulent Viscosity in Relativistic Jets and Accretion Disks

---

**Alexander A. Panferov\***

<sup>a</sup>*Togliatty state university,  
Belorusskaya 14, Togliatty, Russia*

*E-mail:* [panfs@yandex.ru](mailto:panfs@yandex.ru)

The mechanism of turbulent viscosity is the central question in investigations of turbulence. This is also the case in the accretion disk theory, where turbulence is considered to be responsible for the outward transport of angular momentum in the accretion disk. In turbulent flows, vortices transport momentum over their length scales providing the mechanism of viscosity that is controlled by mass entrainment. We have earlier proposed an entrainment model for the particular case of the relativistic jets in the radio galaxy 3C 31. In this paper, we further constrain the model parameters. The model (in the non-relativistic part) is successfully tested versus experimental and simulation data on the Reynolds stresses of free mixing layers and predicts the Smagorinsky constant  $C_S \approx 0.11$ , which is consistent with the experimental range for shear flows  $C_S \approx 0.1-0.12$ . For accretion disks, the entrainment model allows us to derive the same accretion mass rate as in the Shakura–Sunyaev  $\alpha$ -model without appealing to the turbulent kinematic viscosity  $\nu_t$ , and the viscosity parameter  $\alpha$  derived in the form  $\alpha = -\frac{8}{3}\beta s_T \frac{v_t^2}{c_s^2}$  depends on the power  $s_T$  of the temperature slope along the disk radius,  $T \propto r^{s_T}$ , and quadratically on the turbulent velocity  $v_t$ .

*The Multifaceted Universe: Theory and Observations - 2022 (MUTO2022)*  
23-27 May 2022  
SAO RAS, Nizhny Arkhyz, Russia

---

\*Speaker

## 1. Introduction

In free shear flows, which jets and accretion disks look like, turbulent mixing layers develop and entrain matter from the surrounding irrotational flow by means of large-scale vortices [1, Brown & Roshko 2012]. These vortices determine transverse transport of momentum, i.e., turbulent stress.

The turbulent stress  $\tau$  is usually dubbed as the Reynolds stress ( $R$ ), which is determined by turbulent pulsations of fluid velocity, e.g.  $\tau_{xy} = -\rho \overline{v_x v_y}$  for the  $(xy)$ -component of the turbulent stress tensor, which is supplementary to the stress tensor of the Reynolds equations system, where  $\rho$  is the fluid density,  $v_x$  and  $v_y$  are the  $x$  and  $y$ -components of the fluid fluctuating velocity, respectively, thus  $V_x = \overline{V_x} + v_x$  is the whole  $x$ -component of the velocity. The Reynolds stresses cannot be derived from the system of Reynolds equations because the latter is unclosed. The usual approach to the turbulent stress is local, after Boussinesq, through the kinematic turbulent (eddy) viscosity coefficient  $\nu_t$  and the local mean strain  $\tau_{xy} = -\rho \nu_t \frac{\partial \overline{V_x}}{\partial y}$  in *simple* shear, where the gradient  $\frac{\partial \overline{V_x}}{\partial y}$  is only non-zero. The turbulent viscosity may be modelled as  $\nu_t = \nu_t l_m = l_m^2 \left| \frac{\partial \overline{V_x}}{\partial y} \right|$  using the concept of Prandtl's mixing length  $l_m$ , an empirical parameter. In this way Shakura & Sunyaev [2, thereafter SS73] prescribed the turbulent fluid viscosity as  $\nu_t = \nu_t l_m = \alpha c_s H$  in the  $\alpha$ -model of the accretion disk, where  $\alpha = \frac{\nu_t l_m}{c_s H}$  is the viscosity parameter,  $\nu_t$  the turbulent velocity,  $c_s$  the speed of sound,  $H$  the half thickness of the disk. However, the concept of turbulent viscosity does not represent the mechanism of turbulent stress, when large-scale vortices dominate the momentum transport which determines the stress [1, Brown & Roshko 2012].

In our paper [3, Panferov 2017] we have derived a formula for the entrainment in the jets of the radio galaxy 3C 31 (repeated here in Section 2). Here, we express the turbulent shear stress in dependency on turbulence intensity, elaborating the model of Panferov [3], and test this model vs. laboratory and simulation data (Section 3). The model results are successfully applied to explain the experimental value of the Smagorinsky constant, widely used in large eddy simulations of turbulent flows. After this verification we search for entrainment in accretion disks (Section 4). Section 5 is concluding.

## 2. Entrainment in jets of 3C 31

Jets of FR I radio galaxies strongly decelerate at kiloparsec scales [4, Laing and Bridle 2014]. The origin of this is seemingly the turbulent friction of the jets in the ambient medium, which is associated with entrainment and is indicated by a shear at the edges in the transverse velocity profiles of the jets. We have described the profile of the external entrainment along the jet 3C 31 from Wang et al. [5], which is shown in Fig. 1, using the function of mass flux density at the jet edge

$$q_t = \beta \rho_a \nu_t \sigma_t, \quad (1)$$

in dependency on the ambient medium density  $\rho_a$ , the statistical coefficient  $\beta$ , the mean turbulent velocity  $\nu_t$ , and the so-called cross-section of turbulence  $\sigma_t$  [3, Panferov 2017]. In this formula,  $\beta \rho_a \nu_t$  determines the mean flux density of mass in any direction, driven by the turbulence at the

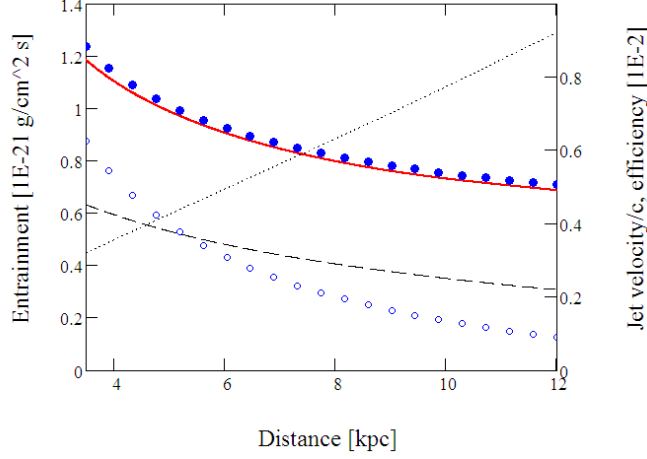


**Figure 1:** Profiles of the entrainment along the jets of 3C 31: for the flux densities of the external (blue solid circles) and internal (blue hollow circles) entrainment according to Wang et al. [5] and the theoretical external entrainment  $q_t$  (red solid line). The internal entrainment is from Fig. 5a of Wang et al. [5], not its approximation  $g_s(x)$ . The jet velocity (dashed line) and the turbulence cross-section (dotted line) are also plotted.

jet edge, and the cross-section

$$\sigma_t = \sin i = \frac{v_{\perp}}{\sqrt{v_{\parallel}^2 + v_{\perp}^2}} = \frac{\eta}{\sqrt{\gamma^2 + \eta^2}} \quad (2)$$

is the efficiency of the capture of matter from vortices, which are imagined as fluid pulsations, by the vortical turbulent flow of the jet of the velocity  $v_j$ . Here  $v_{\parallel} = v_j$ ,  $v_{\perp} = \frac{v_{t\perp}}{\gamma}$  are the parallel and perpendicular components of the velocity (e.g.  $v_{t\perp}^2 = v_y^2 + v_z^2$ ),  $i$  is the inclination to the jet of the turbulence pulses in the jet rest frame,  $\eta = \frac{v_{t\perp}}{v_j}$ ,  $\gamma = \left(1 - \left(\frac{v_j}{c}\right)^2\right)^{-1/2}$  is the Lorentz factor,  $c$  is the speed of light.

Two parameters of the entrainment model,  $\beta$  and  $v_t$ , were defined intuitively as  $\frac{1}{6}$  and the speed of sound  $c_s$ , respectively, and the entrained matter was supposed to just acquire the jet velocity  $v_j$ . The latter supposition straightforwardly gives the turbulent stress at the jet edge  $\tau_t = q_t v_j$ , or  $\tau_t = \alpha P$ , where  $\alpha$  now is the parameter of turbulence intensity, not of turbulent viscosity, and  $P$  is the pressure. Afterwards,  $\beta$  was constrained to  $\frac{1}{5}$  by fitting the function  $q_t$ , which is plotted in Fig. 1, to the external entrainment of Wang et al. [5]. The entrainment model is simple and was compared with very speculative data, therefore its success in this graph seems as miraculous, and further investigations of the model are required.

### 3. Parameters of entrainment model

For isotropical turbulence the mean velocity of stochastical flow in a direction is as follows:

$$v_f = \beta v_t = v_t \int_0^{\pi/2} \cos \theta \frac{2\pi \sin \theta d\theta}{4\pi} = \frac{1}{4} v_t = \frac{1}{4} \sqrt{\frac{3}{2}} v_{\perp}, \quad (3)$$

where  $\theta$  is the inclination of the velocity of pulsation to the given direction. Then Eq. (1) is rewritten as

$$q_t = \beta \rho_a v_{\perp} \sigma_t, \quad (4)$$

where  $\beta = \frac{1}{3.266} \approx \frac{1}{\pi}$  is accepted, and  $v_{\perp}$  substitutes  $v_t$ .

To test this model vs. experimental data on free shear flows, we have to invent how the entrainment  $q_t$  depends on turbulent stresses. For this we define the drag velocity  $v_{\tau}$  so that

$$\tau_{xy} = q_t v_{\tau}, \quad (5)$$

and the mean flux of the fluctuating streamwise momentum  $\rho v_x$  which is transported by the transverse fluctuations  $v_y$ , or the turbulent shear stress, is derived for a self-similar mixing layer as follows:

$$\tau_{xy} = q_t \int_{-\infty}^{y_0} \rho V_x(y)^2 dy \Big/ \int_{-\infty}^{y_0} \rho V_x(y) dy, \quad (6)$$

where  $y_0$  is the depth where  $\tau_{xy}(y_0)$  is maximal, from which we can express  $v_{\tau}$ . Hereafter the term  $V_x$  means the streamwise velocity averaged over time. Hence the drag velocity is the weighted stream velocity acquired by entrained matter, it determines the stress, therefore it substitutes the variable  $v_j$  in the turbulent cross-section (2), as we guess.

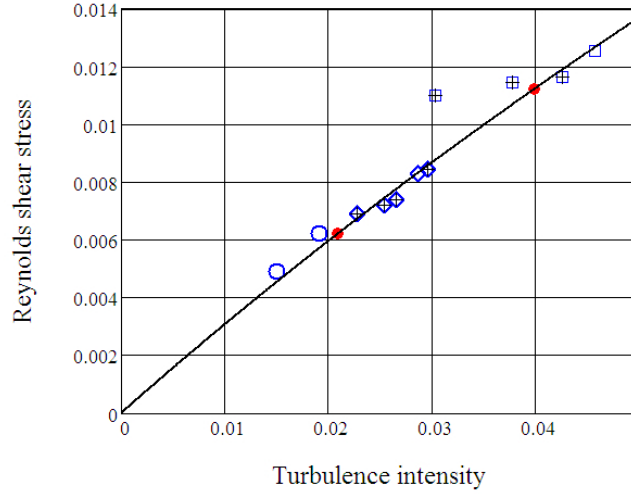


**Figure 2:** A graph of the experimental (red full circles) and simulated (blue hollow symbols) data on the Reynolds stresses of self-similar free mixing layers in coordinates of the squared intensity  $\frac{R_{yy} + R_{zz}}{\rho V_x^2}$  and the normalized shear stress  $\frac{R_{xy}}{\rho V_x^2}$ . The experimental data are from [7, Bell & Mehta 1990] and [8, Gruber et al. 1993], the data of spatial direct numerical simulations (DNS) are from [6, Zhou et al. 2012] and [9, Barre & Bonnet 2015] (circles), the data of variable-density temporal DNS are from [10, Almagro et al. 2017] and [11, Baltzer & Livescu 2020] (squares and diamonds, respectively), crosses stand for the density ratio of the two free streams  $s \neq 1$ . Line is the function  $\tau_{xy} = q_t v_{\tau}$ .

We have collected the experimental and simulated data on the *self-similar* free mixing layers from the literature. To the best of our knowledge, there are only few experimental data on the

needed set of Reynolds stresses ( $R_{xy}$ ,  $R_{yy}$ , and  $R_{zz}$ ): the data on  $R_{zz}$  are very scarce, besides they are contradictory to each other [6, Zhou et al. 2012]. The simulated data on spatial free shear flows also are scarce, and the temporal ones are not quite adequate for the entrainment investigations. The collected data are plotted in Fig. 2 in coordinates of the normalized Reynolds stresses:  $(I_y^2 + I_z^2, I_{xy}^2) \equiv \frac{(R_{yy} + R_{zz}, R_{xy})}{\rho V_x^2}$ , where  $V_x$  is the velocity difference over the shear layer width.

The plot of Eq. (5) is well aligned with the plotted data points and exactly predicts the point of Bell & Mehta. This is the only point among the ocean of experimental data on turbulent mixing layers which is characterized by uncertainty, and this uncertainty is only  $\pm 5\%$ , while the observed experimental scatter is 25-50% for the layer growth rates (and the same is true for the simulations, [12, Smits & Dussauge 2006, pp. 140, 156]). Moreover, this point is the most referenced in comparative studies. Thus, other points have much smaller weights and we don't discuss them.

To take a more hard probe of the entrainment law (4), we checked out its capability to predict the Smagorinsky constant  $C_S$ , an empirical constant used in turbulent flow models in large eddy simulations (e.g. [13, Pope 2000, p. 587]). For a *simple* shear layer we match the kinematic turbulent viscosity after Smagorinsky to the viscosity trivially derived from Eq. (5) omitting the square root in  $\sigma_t$ :

$$\nu_t = (C_S \Delta_S)^2 \left| \frac{dV_x}{dy} \right| \equiv \beta v_\perp^2 \left( \frac{dy}{dV_x} \right)^2 \left| \frac{dV_x}{dy} \right| \approx \beta \left( \frac{v_\perp}{\Delta V_x} \Delta y \right)^2 \left| \frac{dV_x}{dy} \right|, \quad (7)$$

where  $\Delta_S$  is the specific length scale of large eddy simulations, and the mean gradient over the transverse scale  $\Delta y$  substitutes the local gradient. By setting  $\Delta y \equiv \Delta_S$  and substituting the experimental turbulent intensities of self-similar incompressible plane mixing layers from [14, Yoder et al. 2015]

$$0.016 \leq \frac{\overline{v_y^2}}{\Delta V_x^2} \leq 0.020, \quad 0.020 \leq \frac{\overline{v_z^2}}{\Delta V_x^2} \leq 0.022, \quad (8)$$

for the ratio  $\left( \frac{v_\perp}{\Delta V_x} \right)^2$  in Eq. (7) we get the constant value range:

$$C_S = \sqrt{\beta} \frac{v_\perp}{\Delta V_x} = 0.107 - 0.116, \quad (9)$$

which is in the bounds of the experimental range  $C_S \approx 0.1 - 0.12$  for shear flows [15, Sagaut 2006, p. 124]. Omitting of the square root in  $\sigma_t$ , we exaggerated the above  $C_S$  by  $\approx 7\%$ , if to take roughly  $v_\tau = \frac{V_x}{2}$ , it does not change the positivity of our test of the entrainment law vs. the Smagorinsky constant. This justifies the setting  $\Delta y \equiv \Delta_S$  that, on the other hand, suggested proportionality of the scales of turbulent velocity  $\nu_t$  to the driving scales  $\Delta V_x$ , i.e.,  $\frac{v_\perp}{\Delta V_x}$  is independent on  $\Delta y$ .

#### 4. Entrainment in the accretion disk

An accretion disk is a rotating shear layer. Nonlaminar flows are inevitable in accretion disks in view of their huge Reynolds numbers. Pure hydrodynamic turbulence and the formation of even large long-living vortices in accretion disk models have been observed [16, Manger & Klahr

2018]. Vortices, we know, provide turbulent shear stress over macroscopic distances of mixing. We conjecture that long-living shear layers of intermittent vorticity, irrespectively of mechanisms of turbulence, form in the accretion disks (see vorticity maps in [16, Manger & Klahr 2018] and [17, Richard, Nelson & Umurhan 2016]) and entrain the disk matter from the irrotational layers between them, i.e., pull the matter radially inward and outwarf of the disk, with the net effect of matter accretion and angular momentum excretion in the entrainment processes.

In a steady mode of accretion with the accretion rate of mass inflow  $\dot{M}_a$ , the accretion disk between radii  $r$  and  $r_0$  has to shed the angular momentum

$$\dot{M}_a(v_\phi r - v_{\phi 0} r_0) = T_{r\phi} r - T_{r\phi 0} r_0, \quad (10)$$

due to the momentum fluxes  $T_{r\phi}$ . Here  $\dot{M}_a$  and  $T_{r\phi}$  (and the entrainment flux  $Q_t$  below) are the integrated rates over a cylindrical cross-section of the accretion disk of a radius  $r$ , e.g.  $T_{r\phi} = \int_{-\infty}^{\infty} \int_0^{2\pi} \tau_{r\phi} dz d\phi$  in cylindrical coordinates  $(r, \phi, z)$ , and  $v_\phi$  is the azimuthal velocity. Under the condition  $T_{r\phi 0} = 0$ , the momentum flux

$$T_{r\phi} = \dot{M}_a v_\phi \left( 1 - \left( \frac{r}{r_0} \right)^{1/2} \right), \quad (11)$$

which is resolved from Eq. (10) (cf. Eq. (2.4) in [2, SS73], here  $v_\phi$  is allowed to be the Keplerian), can be induced:

- a) either by “the friction between the adjacent layers” [2, SS73], i.e., locally; in this way  $\dot{M}_a$  is derived by Shakura & Sunyaev [2, SS73] as  $\dot{M}_a = f(T_{r\phi})$ ;
- b) or by large-scale vortices, i.e., by entrainment; then  $\dot{M}_a = \Delta Q_t = Q_{t\text{in}} - Q_{t\text{out}}$ , in this way the accretion rate is not a function of turbulent viscosity.

The entrainment in the disk is locally seen as that in a flat mixing layer, for which the formula (4) was designed, if the disk half thickness  $H \ll r$ . For convenience, we again use it in the stripped down version:

$$q_t = \beta \rho \frac{v_\perp^2}{v_\tau}. \quad (12)$$

As in the case discussed above, the fluctuations  $v_\perp$  are proportional to the driving scale  $v_\tau$ , which, again, roughly equals a half of the (Keplerian) velocity difference in the ring turbulent layer of a width  $\Delta r$ . The disk half thickness  $H$  is defined from the disk hydrostatic balance as  $\frac{H}{r} = \frac{c_s}{v_\phi}$ , therefore the drag velocity, and the turbulent velocity  $v_\perp$  too, are scaled with the temperature of the disk as

$$v_\tau = \frac{1}{2} |\Delta v_\phi| \approx \frac{1}{4} \frac{v_\phi}{r} \Delta r = \frac{1}{4} \frac{\Delta r}{H} c_s \propto T^{1/2}. \quad (13)$$

In accretion disks, temperature slopes as  $T \propto r^{s_T}$ , where the power  $s_T < 0$ . The entrainment fluxes  $Q_{t\text{in}}$  and  $Q_{t\text{out}}$  are the time-averages over the same surface but of opposing vortical flows. Here we conjecture that the density of the opposing vortices does not change essentially while they propagate, and their turbulent velocities adjust to the temperature of the ambient medium (really, to the driving velocity, which is the property of the background flow). Thus we get the entrainment

scaling only with  $r$ ,  $q_t \propto r^{s_T/2}$ . Therefore, the accretion rate is derived by a simple difference of the entrainment fluxes  $Q_t$  of the neighboring mixing layers, each of the same width  $\Delta r \ll r$ :

$$\dot{M}_a = 2\pi r \Sigma \beta \left( \frac{v_\perp^2}{v_\tau} \Big|_{r-\Delta r} - \frac{v_\perp^2}{v_\tau} \Big|_{r+\Delta r} \right) \approx -2\pi \Sigma \beta \frac{s_T}{2} \frac{v_\perp^2}{v_\tau} 2\Delta r, \quad (14)$$

where  $\Sigma = \int_{-\infty}^{\infty} \rho dz$  is the surface density in the disk. Substituting expression (13) for  $v_\tau$  in this equation, we arrive to:

$$\dot{M}_a \omega = 2\pi \alpha \Sigma c_s^2, \quad (15)$$

where  $\omega$  is the angular velocity, and

$$\alpha = -\frac{8}{3} \beta s_T \frac{v_t^2}{c_s^2}. \quad (16)$$

The functional form of the accretion rate in Eq. (15) is just the same as in the  $\alpha$ -model of accretion disks of Shakura & Sunyaev [2, SS73, Eq. (2.4)] for  $r \gg r_0$ . Moreover, the viscosity parameter  $\alpha$  has the right functional form  $\alpha \propto \frac{v_t^2}{c_s^2}$ , which can be envisaged from the physical interpretation of the stress  $\tau_{r\phi} \propto \rho v_t^2$  and the definition  $\tau_{r\phi} \propto \alpha \rho c_s^2$  of the parameter  $\alpha$  [2, SS73, Eq. (1.2)].

## 5. Conclusions

We have elucidated the entrainment model of [3, Panferov 2017] and applied it to the problems on turbulent shear stress, in other words, on turbulent viscosity, in a plane mixing layer, in the jets of 3C 31, and in accretion disks. The model reduces the problem of turbulent shear stress to the question about turbulence intensity.

The entrainment model allows us to predict the deceleration of the 3C 31 jets, which is caused by turbulent friction at the jet surface. The model easily expresses the surface turbulent stress in the form  $\tau_t = \alpha P$ , where  $\alpha$  can be set.

Interdependence of the Reynolds stresses observed in plane mixing layers under varying physical conditions is predicted (Fig. 2).

Application of the principles of the entrainment model to the Smagorinsky prescription of turbulent viscosity gave us the Smagorinsky constant  $C_S \simeq 0.11$ , observed in experimental shear flows.

The entrainment model has been shown to be capable to construct the widely used  $\alpha$ -model of accretion disks in another way, bypassing the Prandtl's assignment of turbulent viscosity.

## Acknowledgements

I wish to thank the anonymous referee.

## References

- [1] G. L. Brown and A. Roshko, *Turbulent shear layers and wakes*, *J. Turbulence* **13** (2012) 51

- [2] N. I. Shakura and R. A. Sunyaev, *Black holes in binary systems. Observational appearance*, *Astron. Astrophys.* **24** (1973) 337
- [3] A. Panferov *Jets of SS 433 on scales of dozens of parsecs*, *Astron. Astrophys.* **599** (2017) A77
- [4] R. A. Laing and A. H. Bridle, *Systematic properties of decelerating relativistic jets in low-luminosity radio galaxies*, *Mon. Not. R. Astron. Soc.* **437** (2014) 3405
- [5] Y. Wang, C. R. Kaiser, R. Laing, P. Alexander, G. Pavlovski and C. Knigge, *A relativistic mixing-layer model for jets in low-luminosity radio galaxies*, *Mon. Not. R. Astron. Soc.* **397** (2009) 1113
- [6] Q. Zhou, F. He, M. Y. Shen, *Direct numerical simulation of a spatially developing compressible plane mixing layer: flow structures and mean flow properties*, *J. Fluid Mech.* **711** (2012) 437
- [7] J. H. Bell and R. D. Mehta, *Development of a two-stream mixing layer from tripped and untripped boundary layers*, *AIAA Journal* **28** (1990) 2034
- [8] M. R. Gruber, N. L. Messersmith and J. C. Dutton, *Three-dimensional velocity field in a compressible mixing layer*, *AIAA Journal* **31** (1993) 2061
- [9] S. Barre and J. P. Bonnet, *Detailed experimental study of a highly compressible supersonic turbulent plane mixing layer and comparison with most recent DNS results: Towards an accurate description of compressibility effects in supersonic free shear flows*, *Inter. J. Heat and Fluid Flow* **51** (2015) 324
- [10] A. Almagro, M. Garcia-Villalba and O. Flores, *A numerical study of a variable-density low-speed turbulent mixing layer*, *J. Fluid Mech.* **830** (2017) 569
- [11] J. R. Baltzer and D. Livescu, *Variable-density effects in incompressible non-buoyant shear-driven turbulent mixing layers*, *J. Fluid Mech.* **900** (2020) A16
- [12] A. J. Smits and J.-P. Dussauge, *Turbulent Shear Layers in Supersonic Flow*, Springer Science+Business Media, Inc., New York, 2006
- [13] S. B. Pope, *Turbulent flows*, Cambridge: University Press, 2000
- [14] D. A. Yoder, J. R. DeBonis and N. J. Georgiadis *Modeling of turbulent free shear flows*, *Computers and Fluids* **117** (2015) 212
- [15] P. Sagaut, *Large eddy simulation for incompressible flows: an introduction*, Springer-Verlag Berlin Heidelberg, 2006
- [16] N. Manger and H. Klahr, *Vortex formation and survival in protoplanetary discs subject to vertical shear instability*, *Mon. Not. R. Astron. Soc.* **480** (2018) 2125
- [17] S. Richard, R. P. Nelson and O. M. Umurhan, *Vortex formation in protoplanetary discs induced by the vertical shear instability*, *Mon. Not. R. Astron. Soc.* **456** (2016) 3571